

MGM's JAWAHARLAL NEHRU  
ENGINEERING COLLEGE

# VISTA INTERNATIONAL JOURNAL ON ENERGY, ENVIRONMENT & ENGINEERING



## Comparative study of designed disc rotors using static structural and transient thermal analysis

Mohammad Azar Bargir<sup>1</sup>, Arvind L. Chel<sup>2</sup> and Om M. Raut<sup>3</sup>Assistant Professor<sup>1,3</sup> and Associate Professor<sup>2</sup>Department of Mechanical Engineering,  
MGM's Jawaharlal Nehru Engineering College, Aurangabad, India.

Corresponding author email : azar.bargir@gmail.com Contact:+91-9595940580

### ABSTRACT

Vehicle brakes are one of the most significant safety systems. The function of brakes is based on the conservation of energy. Brakes are used to decelerate the vehicle and eventually stop the vehicle in a certain time and certain distance. Most commonly used brakes are frictional brakes, where the friction produced between two surfaces converts the kinetic energy of the moving vehicle into heat energy. Thermal expansion and stresses are observed in the disk brake rotor at the time of braking, which results in noise and loss of braking effect. Also, performance of brake pads is also affected due to uneven wear.

The objective of this research article is to develop optimized design disc brake rotor by analyzing with Static Structural analysis and Transient thermal analysis using ANSYS 17.0 software. Optimized design of Disc rotor of material AISI 420 stainless steel is manufactured using laser cutting. This study is helpful to reduce the overall total stress, deformation and temperature variation.

**Keywords:** Brake, Rotor, Transient, Static, Thermal, Deformation etc.

### 1. Introduction:

Brake is one of the most important devices of a vehicle used for retarding or stopping the vehicle within smallest possible distance, in consistent with safety and without wheel skidding. The brakes also used to hold the vehicle at rest on an inclined road against the pull of gravity. The brakes must be strong enough to stop the vehicle within a short distance in an emergency but this should be consistent with safety. This is possible only when there is no wheel skidding and driver has proper control over the

vehicle during emergency. The brake must have good anti-fade characteristics i.e. the effectiveness of the brake should be remained constant with prolong application. The degree of reliability of the braking action is directly proportional to the firmness of the entire braking system.

Hence, the rotor is designed to withstand both the maximum possible deceleration and a series of braking cycles. The main problem to deal with in braking cycles is the control of the fading phenomena. High frequency braking cycles lead a rising of the

disc temperature. Therefore, after a period of temperature growth, the disc will reach its balance between the heat generated by braking action and the dissipated heat. At the balance a steady state temperature is reached. If the steady state temperature is too high, several problems happen among which a decay of friction coefficient and a not constant behavior braking. To face this problem, design of disc should focus on disc performances operating with high temperatures (500– 600 oC or more). Discs are then checked on a test bench which simulates extreme braking conditions, such as an alpine downhill or a sport race. [1] The existing disc brake rotor is as shown in Fig.1.

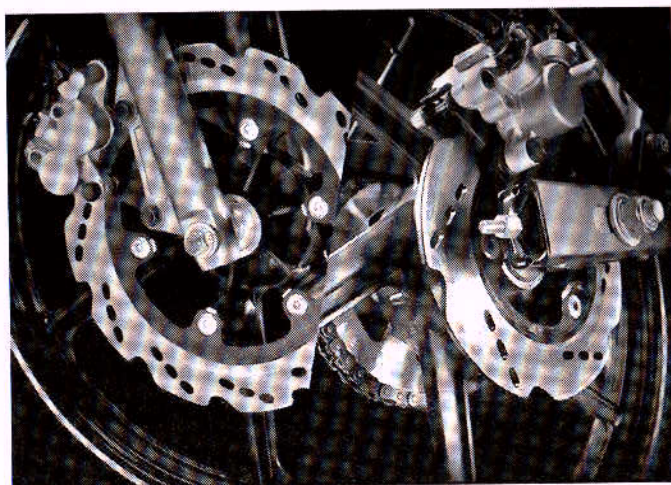


**Fig.1 Existing disc brake rotor of AISI 420 Stainless Steel [2]**

**2. Selection of Material AISI 420 SS for Disc Rotor:**

The properties of types of material used for manufacturing disc rotor as mentioned in the Table 1, Stainless Steel (AISI-420) has better properties than other materials. The selected Material is Stainless Steel (AISI-420) and its properties are tested on spectrometer

**Table 1. Properties of Materials used for Disc Brake Rotor [3]**

Properties	Types of material used for Disc Brake Rotor			
	Stainless Steel	Grey Cast iron	AL MMC	E Glass
Density,	7850 Kg/m <sup>3</sup>	7.2gm/m <sup>3</sup>	3.98gm/m <sup>3</sup>	2.6mg/m <sup>3</sup>
Young modulus, E	200 GPa	97GPa	380GPa	85GPa
Thermal conductivity	24.9 W/m-k	46 W/m-k	31W/m-k	1.35 W/m-k
Specific heat,	460 J/Kg-k	450 J/Kg-k	250J/Kg-k	805J/Kg-k
Poission's ratio	0.3	0.25	0.22	0.23

**3. Designing of disc brake rotor:**

The manufacturing of new design disc work is done on the existing disc and modified it with some changes like cut patterns and with new profiles. The existing disc is designed using CATIA software as shown in Fig.2. This existing disc is compared finally with newly designed disc rotor on CATIA V5as shown in Fig. 3. Analysis of existing disc and new developed disc model is done using ANSYS. Three results are compared from existing disc with five new models. Existing disc rotor profile has parametric cuts and elliptical holes instead of circular holes. The elliptical holes are used to reduce the stress concentration.

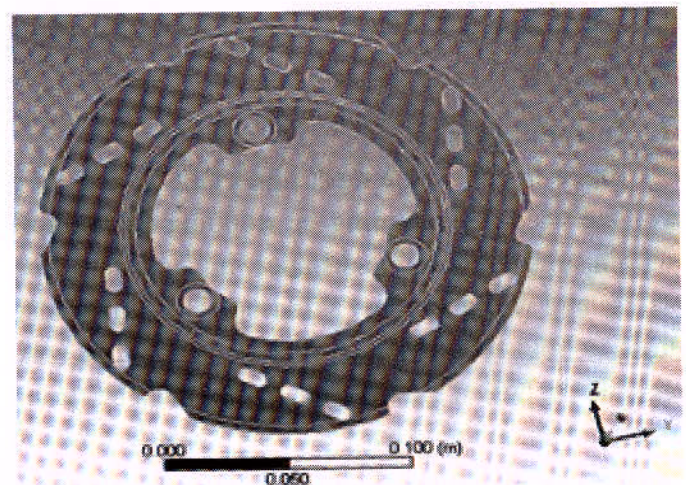


**Fig. 2 Design on CATIA V5 of existing disc brake rotor**

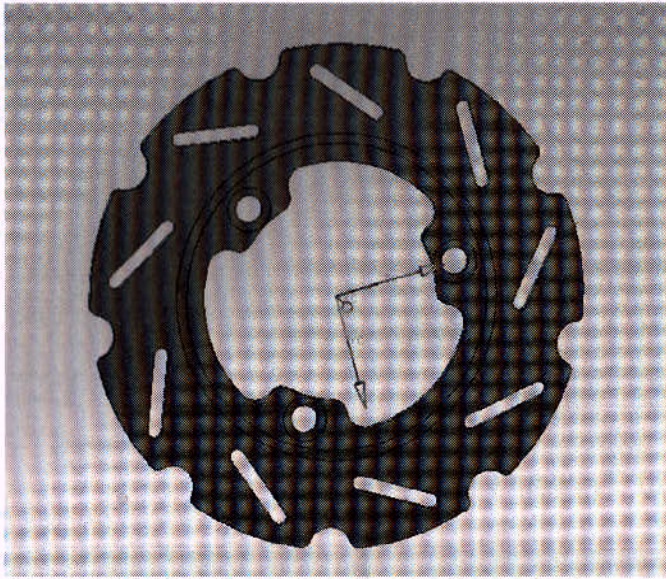


**Fig. 3 Newly designed disc rotor using CATIA V5**

**4. Proposed Counter measures in Design**

In Specimen, counter measures in design are made by reducing number of piercing holes without changing the orientation of holes. The piercing holes act as stress raisers which lead to localized high stresses. It is possible to reduce the maximum stress value by changing its profile geometry. The holes in the brake-disk can be assumed to behave like elliptical cracks in a structure. Elliptical cracks under tensile loading would raise the value of yield stress [4] to

$$\sigma_y = S [1 + 2 (C/D)]$$

Stress at cracks can be given by  $\sigma_y = k_t \cdot \sigma_{normal}$

where  $k_t$  is the stress concentration factor for elliptical cracks

Hence,

For a circle,  $a = b$ ,  $k_t = 3$

For an ellipse of  $a/b=3$ ,  $k_t = 1.67$

It is important to remember that stress amplification not only occurs on a microscopic level (e.g. small flaws or cracks,) but it can also occur on the

macroscopic level in the case of sharp corners, holes, fillets, and notches. Hence, this basic theory can be applied to the piercing holes in the brake-disk. The variation of stress concentration of an elliptical hole is as shown in Fig.4.

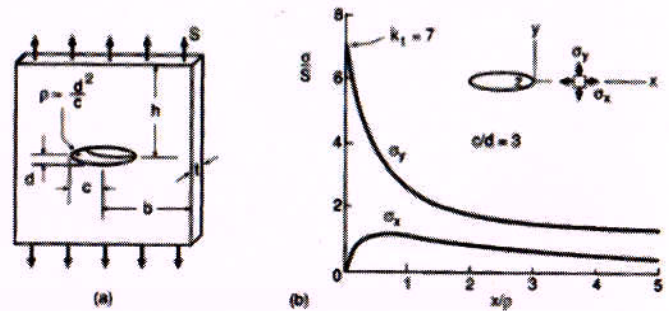


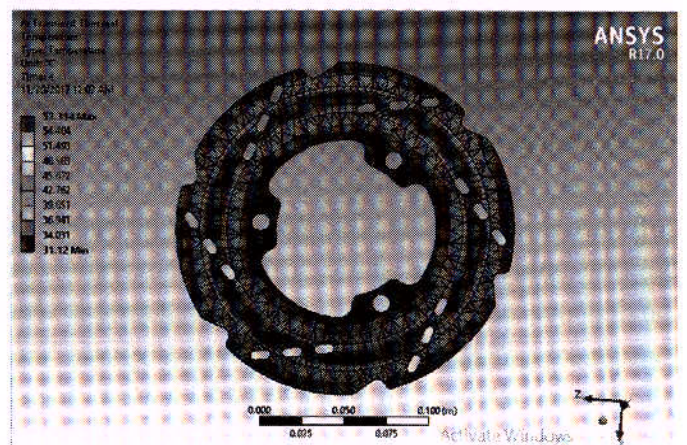
**Fig. 4. Stress at an elliptical hole [4]**

**5. Analysis in ANSYS of Disc Rotors:**

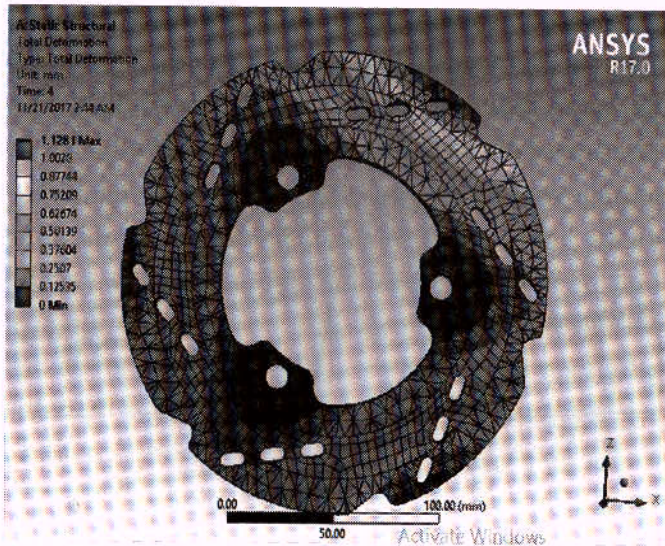
**5.1 Transient thermal and static analysis of the existing disc rotor:**

The various parameters analyzed in this research are temperature, total deformation and structural and thermal stresses. These stresses are induced while application of brake. Existing disc rotor modeled in CATIA was imported in ANSYS R17.0.

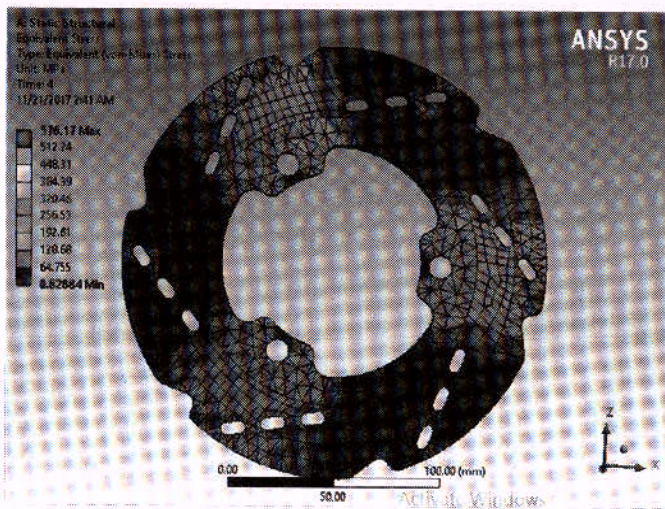
Transient thermal analysis and static structural analysis were carried out. The results obtained for the existing disc rotor using thermal analysis are maximum temperature 57.3°C Fig.5.(a), total deformation 1.13 mm Fig.5(b) and maximum thermal Stress 576.17 MPa Fig.5(c).



**(a) Temperature distribution**



(b) Total deformation

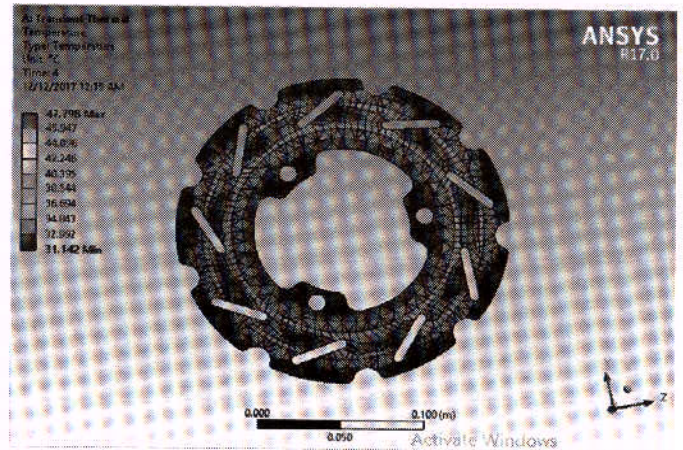


(c) Thermal stress

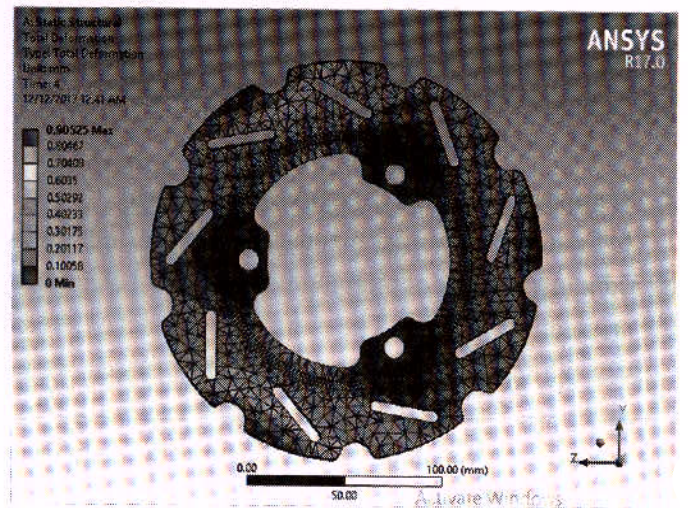
**Fig.5** Thermal analysis of existing disc rotor (a) temperature (b) deformation (c) stress

**5.2 Transient thermal and static analysis of the newly designed disc rotor:**

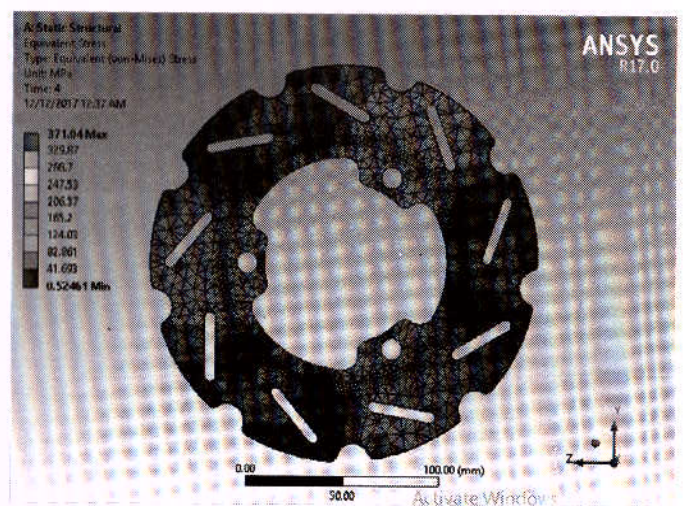
Newly designed disc rotor modeled CATIA software is imported in ANSYS R17.0. The transient thermal analysis and static structural analysis was carried out on this new designed disc rotor. The results obtained from the thermal analysis are maximum temperature 47.8°C Fig.6(a), total deformation 0.9 mm Fig.6(b) and maximum thermal stress 371.04 MPa Fig.6(c).



(a) Temperature distribution



(b) Total deformation



(c) Thermal stress

**Fig.6** Thermal analysis of newly designed disc rotor (a) temperature (b) deformation (c) stress

### 5.3 Result of Transient Thermal and Static Analysis:

Table 2 gives the significant result obtained based on the transient thermal and static analysis of existing and newly designed disc rotor.

**Table 2.** Result of transient thermal and static analysis of existing and designed disc rotors

DISC	Temp (°C)	Equivalent Stresses (MPa)	Total Deformation (mm)
Existing Disc Rotor	57.314	576.17	1.128
Designed Disc Rotor	47.798	371.04	0.905

## 6. Manufacturing of newly designed disc rotor using laser cutting machine

The designed disc rotor was manufactured using laser cutting machine as shown in Fig.7.



**Fig.7 Laser cutting machine for designed disc rotor (Mazak Turbo X-48 Champion)**

### 6.1 Design and functions:

During laser beam cutting, the distance between nozzle and work-piece may unintentionally vary. This is caused by thermal stress and work-piece form tolerances. Optimum cutting quality and cutting speed are only achieved when cutting nozzle and focus are positioned correctly in relation to the work-

piece surface. Deviations of just a few tenths of a millimeter can lead to burr formation and negatively affect the cutting speed, the roughness of the cutting surfaces and kerf width.

The Laser system enables precise distance control at high cutting speed. The distance to the work-piece surface is detected by means of capacitive distance sensors in the cutting head. A preamplifier transmits the sensor signal to the adjust box. This analyses the signal. The output signal can then be used to control a linear drive. [4]

### 6.2 Control voltage, distance signal:

The adjust box optionally delivers an analogue control voltage or a linear distance signal. The PID-parameters of the control signal can be programmed on the adjust box.

### 6.3 Standoff distance:

The adjust box measures distances with a resolution of max. 0.1% of the measuring range limits (MBEW). The measuring signal is digitalized, linearized and transmitted to a digital PID controller. The controller provides a control voltage of  $\pm 10$  V to control a servo drive. The system continuously monitors the set point position. When the set point position is reached, 'POS.REACHED' is output if the position is within the programmed set point range.

### 6.4 External standoff distance (I/O interface):

The standoff distance can also be set via an external, analogue signal (0 V to 10 V). Voltage values between 0.3 V and 9.7 V correspond to a standoff distance of 3% and 97% of the measuring range limit (MBEW). A microcontroller continuously checks the control system and the proper functioning of the device. The integrated I/O interface with electric isolation enables the device to be connected to a CNC/PLC controller.

### 6.5 Characteristic curves:

Cutting heads use different measuring principles and thus have different nonlinear characteristic curves. The adjust box enables you to calibrate and manage characteristic curves. Two different operating

modes can be selected:

## 7. Operating mode of laser cutting machine:

### 7.1 Default characteristic curves:

In this operating mode, you can select the characteristic curve that best suits your sensor from 8 default curves. The sensor is first moved to the measuring range limit. Then the limit value is calibrated using 'SET RANGE'. After limit value calibration, the flattest of the 8 characteristic curves is enabled. In order to obtain a characteristic curve that suits the process better, the cutting head is moved to a distance of 1 mm and the best characteristic curve is selected using 'SELECT CHAR.BIT0'. Then the system automatically adds an internal offset to this characteristic curve to create an output voltage of 1 volt. If a voltage is applied that exceeds these limits, the adjusted value of the device is valid. You should consider this behavior when programming the controller distance of 1 mm. As only fixed (default) characteristic curves can be selected, higher or smaller deviations from the ideal characteristic curve cannot be avoided. This operating mode is particularly useful for setting up the system quickly, for linear drive units that cannot be positioned and when linearization is carried out by the controller. If the controller line arise the characteristic curve, you should only calibrate the measuring range limit in order to obtain the highest possible cutting distance resolution [3].

### 7.2 User characteristic curves:

In this operating mode, the adjust box calibrates the cutting head sensor. The sensor's measuring range values are approached one after the other. The results are then saved in the device. Up to 8 individual characteristic curves can thus be learned. Applying combination to the digital inputs, these characteristic curves can be enabled. This function is particularly useful when different setting angles are used during cutting or when cutting close to the sheet edge, as the characteristic curves can be enabled quickly. The operating mode "User characteristic curves" enables

the process to be adapted to the sensor geometry with utmost precision. The machine controller can approach the reference points. Digital I/O signals are used to carry out calibration automatically. Select this high precision operating mode if the machine controller can position the linear drive.

### 7.3 Procedure of cutting of disc on Laser cutting machine:

#### 7.3.1 Model drawing of Auto-CAD:

First model is prepared on the Auto-CAD. According to given drawing the program is prepared. The drawing and program is feed in Laser cutting machine unit (i.e. computer). The cutting speed of spindle of Laser cutter is kept minimum to avoid bending of plate and to get better finishing. Fig.8 shows the cutting disc rotor on laser cutting machine. The designed disc rotor was manufactured using laser cutting as shown in Fig.9.

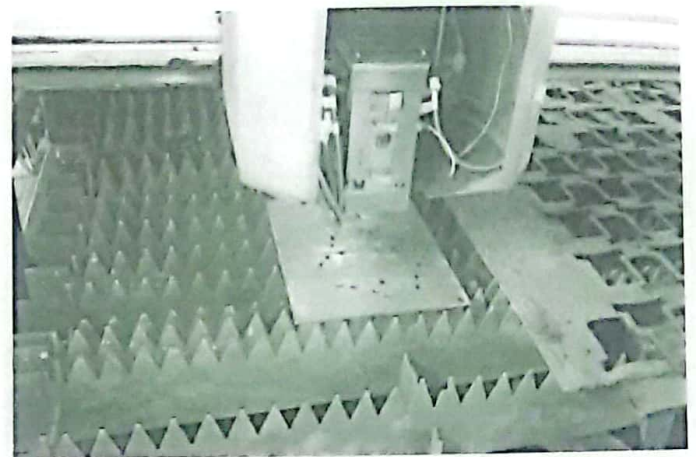


Fig.8 Cutting of disc on Laser cutting machine

#### 7.3.2 Drilling and counter boring:

Three counter holes are drill-using drill bit 17 mm diameter up to depth of 2mm for fitting purpose of disc on the wheel axle.



**Fig.9 Designed disc rotor manufactured after Laser Cutting**

## 8. Conclusion:

The three-dimensional modelling and meshing using FEA method were successfully implemented in the analysis presented in this paper. The disc rotor was designed by varying cut patterns and providing cuts to diameter in order to reduce weight of rotor, changing orientations of holes and replacing circular holes to elliptical holes. The results have shown that by combining pierced holes, there is reduction in the stress concentration. Results from the analysis namely maximum disc temperature, total deformation and thermal stresses were obtained and found to be below the existing disc rotor (Table 2). In case of the existing disc rotor design the maximum temperature is 57.314 °C for one braking cycle of 4 seconds subjected to the pressure of 1 MPa, whereas the newly designed disc rotor reaches with maximum temperature of 47.798°C under same boundary conditions. Thermal Stresses induced in existing disc rotor is 576.17 MPa comparatively higher than thermal stresses induced in designed disc rotor (371.04 MPa).

The analysis was carried out successfully using

transient thermal and static structural analysis of both disc rotors existing used disc rotor in the vehicle and designed disc rotor. The newly designed disc rotor gives improved results than the existing disc rotor considering all parameters. Hence, the designed disc is manufactured using laser cutting operation explained in this research for basic understanding to the users.

## Acknowledgement:

Authors thank the Management of Aakar Laser Cutting Tools for providing an opportunity to work on the Factory setup of Laser Cutting Machine at Aakar Laser Cutting, Plot No- W 322, Rabale MIDC, Navi Mumbai, Dist.Thane, Rabale, Navi Mumbai, Pin 400701.

## 9. References:

- [1] Manjunath T.V. and Suresh P M. (2013), Structural and Thermal Analysis of Rotor Disc of Disc Brake, International Journal of Innovative Research in Science, Engineering and Technology 2(12), 7741-7749.
- [2] Reddy V.C., Reddy M.G. and Gowd G.H., (2013), Modelling and Analysis of FSAE Car Disc Brake Using FEM, International Journal of Emerging Technology and Advanced Engineering, 3(9), 383-389.
- [3] Reddy N., Reddy K., Balaji N. Ganesh, 2013, Design, Structural and Thermal Analysis of Disc Brake, International Journal of Futuristic Science Engineering and Technology, 1(3), 167-171.
- [4] Zhiyong Y., Jianmin H., Weijing L., Zhiqiang L., Pan L., Shi X. (2013), Analyzing the mechanisms of fatigue crack initiation and propagation in CRH EMU brake discs, Engineering Failure Analysis, 34, 121-128.